

# Hybrid feedback control for path tracking with a bounded-curvature vehicle <sup>★</sup>

Andrea Balluchi<sup>1</sup>, Philippe Souères<sup>2</sup>, and Antonio Bicchi<sup>3</sup>

<sup>1</sup> PARADES, Via di S.Pantaleo, 66, 00186 Roma, Italy.

`balluchi@parades.rm.cnr.it`

<sup>2</sup> Laboratoire d'Analyse et d'Architecture des Systèmes – LAAS, CNRS, 7, Avenue du Colonel Roche, 31077 Toulouse, France. `soueres@laas.fr`

<sup>3</sup> Centro Interdipartimentale di Ricerca “Enrico Piaggio”. Università di Pisa, 56100 Pisa, Italy, `bicchi@ing.unipi.it`

**Abstract.** In this paper, we consider the problem of stabilizing the kinematic model of a car to a general path in the plane, subject to very mild restrictions. The car model, although rather simplified, contains some of the most relevant limitations that make application of existing results in the literature impossible: namely, the car can only move forward, and turn with a bounded steering radius; also, only limited sensory information is available.

The approach we follow to stabilization is to adapt to the present general case an optimal synthesis approach successfully applied in our previous work to tracking rectilinear paths. Due to both the nature of the problem, and the solution technique used, the analysis of the controlled system involves a rather complex switching logic. Hybrid formalism and verification techniques prove extremely useful in this context to formally prove stability of the resulting system, and are described in detail in the paper.

## 1 Introduction

In this paper we consider the design of a control law for path tracking by a so-called Dubins' model of a car. Dubins' cars are kinematic models of wheeled (nonholonomic) vehicles that move only forward in a plane, and possess a lower-bounded turning radius. The model is relevant to the kinematics of road vehicles as well as aircraft cruising at constant altitude, or sea vessels.

Although the design of control techniques for nonholonomic vehicles has been the subject of extensive research recently (see e.g. [10, 12, 6]), the additional constraint that the steering radius of the vehicle is lower bounded has not been explicitly considered. However, such a restriction appears to be crucial in making a kinematic model of a car relevant to real-world vehicles encountered in most applications. Another important assumption often used in the literature is that the full state of the system is available for measurement, and that the path to

---

<sup>★</sup> The work has been conducted with partial support of PARADES, a Cadence, Magneti-Marelli and ST-microelectronics E.E.I.G, by CNR PF-MADESSII SP3.1.2.

be tracked is entirely known in advance. Instead, we consider in this paper the more realistic and less demanding case that the vehicle can only measure its current distance and heading angle error with respect to the closest point on the reference path in the plane, where only the sign of the path curvature is detected.

The approach we follow to stabilization of Dubins' cars is to adapt to the present general case an optimal synthesis approach successfully applied in our previous work to tracking rectilinear paths [11]. Due to both the nature of the problem, the type of sensors, and the solution technique used, the analysis of the controlled system involves a rather complex switching logic. Hybrid formalism (see [5, 14, 2]) and verification techniques (see [8, 7, 1]) prove extremely useful in this context to formally proof stability of the resulting system, and are described in detail in the paper, which is organized as follows.

In Section 2, a hybrid automaton that describes the motion of the vehicle with respect to the path is introduced, while in Section 3 the path-tracking controller is developed. Such controller, described in detail in Section 3.2, is obtained by considering a local approximation of the desired path with the tangent line, and by using a feedback controller designed for stabilization on straight paths (reported in Section 3.1). The advantages of the novel hybrid path-tracking formalization are exploited in Section 4, where the stability properties of the proposed controller are investigated. By a reachability analysis in the continuous state space, a finite state abstract representation of the hybrid closed-loop automaton is obtained. Though this representation is not a bisimulation, but rather a simulation, of the hybrid automaton ([5]), it suffices to prove the stability properties of the proposed control. It is shown that the proposed hybrid feedback controller achieves stabilization of the Dubins' car on a generic reference path and sufficient conditions for global attractivity are derived.

## 2 Hybrid path tracking modeling using switching Frenet frames

We consider the kinematic model of a car-like robot moving forward on a plane, which was introduced by Dubins in [4]. A configuration of the vehicle is defined by an ordered pair  $(M(x, y), \theta) \in \mathbb{R}^2 \times S^1$ , where  $(x, y)$  are the coordinates of a reference point  $M$  in the plane and  $\theta$  is the angle made by the direction of the robot with respect to the  $x$ -axis. The kinematics of the car are described by

$$\begin{cases} \dot{x} = V \cos \theta \\ \dot{y} = V \sin \theta \\ \dot{\theta} = \omega \end{cases} \quad \text{with} \quad |\omega| < \frac{V}{R} \quad (1)$$

where  $V$  is the constant forward velocity,  $\omega$  the is turning speed and the input constraint models a lower bound  $R > 0$  on the turning radius of the car.

The problem we are concerned with is that of steering the vehicle to a given *feasible* path  $\Gamma$ , defined in the arclength parametrization by

$$\Gamma = \{(\hat{x}, \hat{y}) \in \mathbb{R}^2 \mid (\hat{x}, \hat{y}) = \hat{g}(\beta) \text{ for } \beta \in \mathbb{R}\} \quad (2)$$

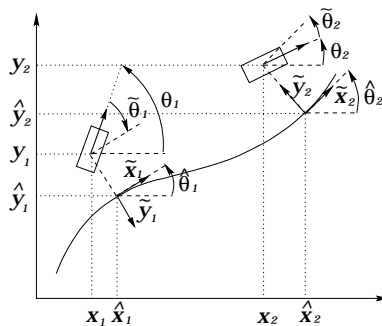


Fig. 1. Reference path and transformed coordinates.

with the following conditions:

- A)  $\hat{g}(\cdot)$  is a class  $C^1$  mapping from  $\mathbb{R}$  to  $\mathbb{R}^2$  and the orientation of  $\Gamma$  is that induced by increasing  $\beta$ ;
- B) Denoting by  $\kappa(\beta)$  the curvature of  $\Gamma$  at  $\hat{g}(\beta)$  for all  $\beta \in \mathbb{R}$  where it is well-defined and setting  $\kappa(\beta) = \lim_{s \rightarrow \beta^-} \kappa(s)$ , when  $\kappa(\beta)$  is not well-defined, there exists a positive real  $R_\Gamma$  such that the normalized curvature  $\hat{\kappa}(s) \equiv R\kappa(s)$  satisfies

$$|\hat{\kappa}(\beta)| = R|\kappa(\beta)| \leq \frac{R}{R_\Gamma} \equiv C < 1. \quad (3)$$

- C) Considering the open neighborhood of the path

$$\mathcal{T}_\Gamma = \{\mathbf{x} \in \mathbb{R}^2 : \exists \beta \in \mathbb{R}, \|\mathbf{x} - \hat{g}(\beta)\| < R_\Gamma\} \subset \mathbb{R}^2, \quad (4)$$

for all  $\mathbf{x} \in \mathcal{T}_\Gamma$  there exists a unique nearest point on  $\Gamma$ .

In order to describe the motion of the vehicle with respect to the reference path  $\Gamma$  a mobile Frenet's frame associated to the curve  $\Gamma$  is considered. Given a vehicle position  $M(x, y) \in \mathcal{T}_\Gamma$ , the Frenet's frame  $\mathcal{S}_T(s)|_{s=\bar{\beta}}$  is defined by the tangent, the principal normal and the binormal axes of the curve at the point  $(\hat{x}(\bar{\beta}), \hat{y}(\bar{\beta}))$  of  $\Gamma$ , located at the minimum distance<sup>1</sup> from  $M(x, y)$  (see Figure 1). As the vehicle moves with velocity  $V$ , the Frenet's frame  $\mathcal{S}_T(s)$  follows its motion so as to keep it on the principal normal axis. The arclength abscissa  $s$  locates the current Frenet's frame. The tangent and the principal normal axes of  $\mathcal{S}_T(s)$  remain within the plane containing the curve, while the binormal axis points either upwards, if the local curvature of  $\Gamma$  is counterclockwise (i.e.  $\kappa(s) > 0$ ), or downwards, if the local curvature is clockwise (i.e.  $\kappa(s) < 0$ ). Introduce the transformed coordinates  $(s, \tilde{y}, \tilde{\theta})$ , where:

- abscissa  $s$  defines the position of the Frenet's frame along the curve;

<sup>1</sup> Note that, by assumptions A), B) and C) the Frenet's frame is well-defined along  $\Gamma$ .

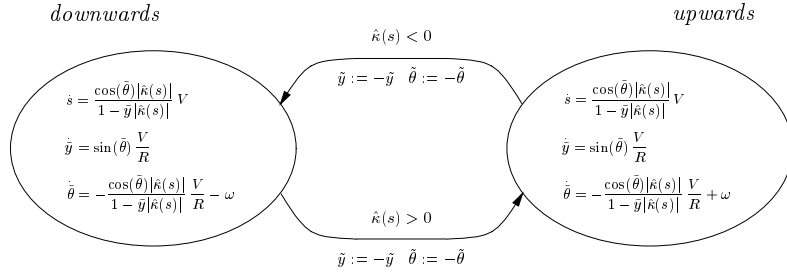


**Fig. 2.** Hybrid automaton  $PTHA_2$  modeling the car in the transformed state space.

- $\tilde{y}$  denotes the position of the robot along the principal normal of  $\mathcal{S}_T(s)$  (lateral distance) normalized with respect to the minimum turning radius  $R$ ;
- $\tilde{\theta}$  denotes its orientation with respect to the tangent axis of  $\mathcal{S}_T(s)$  (heading angle error), with sign taken according to the local direction of the binormal axis (see Figure 1).

It can be noticed that this coordinate system is similar to the one used by Samson [9], except for the switchings of the Frenet's frame. In fact, a change of curvature along the path produces a jump of the variables  $\tilde{y}$  and  $\tilde{\theta}$  to the symmetric point with respect to the origin in the  $(\tilde{y}, \tilde{\theta})$ -plane. The reason for introducing such discontinuity in the model is related to the different behaviors that a vehicle with bounded curvature has when it approaches a reference path. Indeed, the approach is apparently easier if the vehicle and the center of curvature of the path lie on the opposite sides of the curve<sup>2</sup>. This formulation will turn out to be useful in the verification of the proposed path tracking controller.

The motion of the robot in the transformed state  $(s, \tilde{y}, \tilde{\theta})^T$  can be described by using the formalism of hybrid automata (see [5, 3]). The discrete nature of the model arises from the fact that the Frenet's frame  $\mathcal{S}_T(s)$  changes its orientation during the motion, depending on the sign of the curvature  $\hat{\kappa}(s)$ . The discrete state, referred to as *bin*, assumes values in the set  $\{\text{upwards}, \text{downwards}\}$ , where *upwards* and *downwards* stands, respectively, for a upwards and downwards binormal axis of  $\mathcal{S}_T(s(t))$ , at time  $t$ . The initial mode *bin* is: *upwards*, if  $\hat{\kappa}(s(0)) > 0$ ; *downwards*, if  $\hat{\kappa}(s(0)) < 0$ ; and any of those, otherwise. The dynamics the continuous states are subject to, in any open interval of time where the sign of  $\hat{\kappa}(s(t))$  does not change, are obtained by geometric arguments. The complete Path-Tracking Hybrid Automaton, referred to as  $PTHA_2$ , is depicted in Figure 2.

The specification for the design of a path tracking controller for the Dubins' car can be formulated using the hybrid automaton  $PTHA_2$ , which captures the

<sup>2</sup> For instance, if the vehicle is required to approach a circle with curvature  $1/R$ , then it can approach it only from outside.

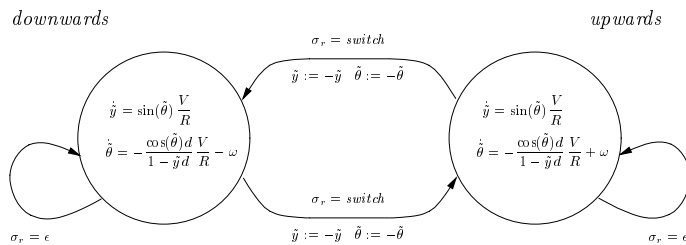


**Fig. 3.** Hybrid automaton  $PTHA_2$  of the vehicle in the reduced state space.

different behaviors of the bounded-curvature vehicle in approaching the path. For such hybrid model, the problem reduces to that one of steering  $(\tilde{y}, \tilde{\theta})$  to  $(0, 0)$ .

Assuming that only the sign of  $\hat{\kappa}(s)$  is available but not its amplitude, a reduced hybrid automaton can be considered for the path tracking problem. The local curvature  $|\hat{\kappa}(s)|$  is replaced by an unknown input disturbance  $d(t)$  the path tracking controller has to be robust to. By (3), disturbance  $d(t)$  satisfies

$$0 \leq d(t) \leq C < 1. \quad (5)$$

The path tracking problem is described in the reduced continuous state space  $(\tilde{y}, \tilde{\theta})$ . Curvature sign switching conditions  $\hat{\kappa}(s) > 0$  and  $\hat{\kappa}(s) < 0$  are modeled by a discrete uncontrollable input  $\sigma_r$  assuming either *switch* (when a change of curvature sign occurs) or the *silent move*  $\epsilon$  (otherwise). The reduced hybrid automaton, referred to as  $PTHA_2$ , is reported in Figure 3.

In this case the path tracking problem is formulated as follows:

*Problem 1.* Let  $\Gamma$  as in (2) be a feasible reference path. Given the hybrid automaton  $PTHA_2$ , find a feedback control law  $\omega(bin, (\tilde{y}, \tilde{\theta}))$  satisfying curvature constraint (1) such that, from any initial state  $(bin_0, (\tilde{y}_0, \tilde{\theta}_0))$  the trajectory  $(\tilde{y}(t), \tilde{\theta}(t))$  converges to the origin under the action of any unknown disturbance  $d(t)$ , bounded as in (5), and any sequence of uncontrollable events  $\sigma_r$ .

### 3 Hybrid path-tracking feedback controller

#### 3.1 Optimal feedback control for line tracking

In [11], the problem of driving the Dubins' car to a straight path has been considered. An optimal feedback control that minimizes the length travelled by the vehicle to reach the specified path was devised. Define  $\sigma_N(\tilde{y}, \tilde{\theta}) = \tilde{y} + 1 + \cos(\tilde{\theta})$  and  $\sigma_P(\tilde{y}, \tilde{\theta}) = \tilde{y} - 1 - \cos(\tilde{\theta})$ . The optimal feedback control presented

in [11] is defined inside the region

$$\mathcal{D}_{(\tilde{y}, \tilde{\theta})} = \begin{cases} \sigma_N(\tilde{y}, \tilde{\theta}) < 0 \wedge \tilde{\theta} \in [\pi, \frac{3}{2}\pi) \vee \\ \sigma_P(\tilde{y}, \tilde{\theta}) \leq 0 \wedge \tilde{\theta} \in (\frac{\pi}{2}, \pi) \vee \\ \tilde{\theta} \in [-\frac{\pi}{2}, \frac{\pi}{2}] \vee \\ \sigma_N(\tilde{y}, \tilde{\theta}) \geq 0 \wedge \tilde{\theta} \in [-\pi, -\frac{\pi}{2}) \vee \\ \sigma_P(\tilde{y}, \tilde{\theta}) > 0 \wedge \tilde{\theta} \in (-\frac{3}{2}\pi, -\pi) \end{cases} \quad (6)$$

in the state space  $(\tilde{y}, \tilde{\theta})$ , which, modulo  $2\pi$  angles on  $\tilde{\theta}$ , corresponds to the whole space (see Figure 5). The optimal controller is described by three modes,

$\Omega^0 = \mathbf{sr} \cup \mathbf{sl} \cup \mathbf{O}, \quad \Omega^- = \mathbf{r} \cup \mathbf{rsr} \cup \mathbf{rsl} \cup \mathbf{rl}^{(1)} \cup \mathbf{rl}^{(2)}, \quad \Omega^+ = \mathbf{l} \cup \mathbf{lsr} \cup \mathbf{lsl} \cup \mathbf{lr}^{(1)} \cup \mathbf{lr}^{(2)}, \quad \mathbf{O} = \{(0, 0)\}$ $\mathbf{r} = \mathbf{r}^{(1)} \cup \mathbf{r}^{(2)} \cup \mathbf{r}^{(3)}, \quad \mathbf{lr}^{(1)} = \mathbf{lr}^{(1.1)} \cup \mathbf{lr}^{(1.2)} \cup \mathbf{lr}^{(1.3)}, \quad \mathbf{lsr} = \mathbf{lsr}^{(1)} \cup \mathbf{lsr}^{(2)}, \quad \mathbf{rsr} = \mathbf{rsr}^{(1)} \cup \mathbf{rsr}^{(2)}$ $\mathbf{l} = \mathbf{l}^{(1)} \cup \mathbf{l}^{(2)} \cup \mathbf{l}^{(3)}, \quad \mathbf{rl}^{(1)} = \mathbf{rl}^{(1.1)} \cup \mathbf{rl}^{(1.2)} \cup \mathbf{rl}^{(1.3)}, \quad \mathbf{rsl} = \mathbf{rsl}^{(1)} \cup \mathbf{rsl}^{(2)}, \quad \mathbf{lsl} = \mathbf{lsl}^{(1)} \cup \mathbf{lsl}^{(2)}$	
$\mathbf{r}^{(1)} = \{(\tilde{y}, \tilde{\theta})   \tilde{\theta} \in (0, \frac{\pi}{2}), \sigma_R(\tilde{y}, \tilde{\theta}) = 0\},$ $\mathbf{r}^{(2)} = \{(\tilde{y}, \tilde{\theta})   \tilde{\theta} \in [\frac{\pi}{2}, \pi), \sigma_R(\tilde{y}, \tilde{\theta}) = 0\},$ $\mathbf{r}^{(3)} = \{(\tilde{y}, \tilde{\theta})   \tilde{\theta} \in [\pi, \frac{3}{2}\pi), \sigma_R(\tilde{y}, \tilde{\theta}) = 0\} \cup \{(0, \pi)\}$ $\mathbf{lr}^{(1.1)} = \{(\tilde{y}, \tilde{\theta})   \tilde{\theta} \in (0, \frac{\pi}{2}), \sigma_N(\tilde{y}, \tilde{\theta}) \geq 0, \sigma_L(\tilde{y}, \tilde{\theta}) < 0\}$ $\mathbf{lr}^{(1.2)} = \{(\tilde{y}, \tilde{\theta})   \tilde{\theta} \in (-\frac{\pi}{2}, 0), \sigma_N(\tilde{y}, \tilde{\theta}) \geq 0, \sigma_R(\tilde{y}, \tilde{\theta}) < 0\}$ $\mathbf{lr}^{(1.3)} = \{(\tilde{y}, \tilde{\theta})   \tilde{\theta} \in (-\pi, -\frac{\pi}{2}), \sigma_N(\tilde{y}, \tilde{\theta}) \geq 0, \sigma_R(\tilde{y}, \tilde{\theta}) < 0\}$ $\mathbf{lr}^{(2)} = \{(\tilde{y}, \tilde{\theta})   \tilde{\theta} \in [\pi, \frac{3}{2}\pi), \sigma_R(\tilde{y}, \tilde{\theta}) > 0, \sigma_N(\tilde{y}, \tilde{\theta}) < 0\}$ $\mathbf{sr} = \{(\tilde{y}, \tilde{\theta})   \tilde{y} < -1, \tilde{\theta} = \frac{\pi}{2}\}$ $\mathbf{lsr}^{(1)} = \{(\tilde{y}, \tilde{\theta})   \tilde{\theta} \in [0, \frac{\pi}{2}), \sigma_N(\tilde{y}, \tilde{\theta}) < 0\}$ $\mathbf{lsr}^{(2)} = \{(\tilde{y}, \tilde{\theta})   \tilde{\theta} \in [-\frac{\pi}{2}, 0), \sigma_N(\tilde{y}, \tilde{\theta}) < 0\}$ $\mathbf{rsr}^{(1)} = \{(\tilde{y}, \tilde{\theta})   \tilde{\theta} \in (\frac{\pi}{2}, \pi), \sigma_R(\tilde{y}, \tilde{\theta}) < 0\}$ $\mathbf{rsr}^{(2)} = \{(\tilde{y}, \tilde{\theta})   \tilde{\theta} \in [\pi, \frac{3}{2}\pi), \sigma_R(\tilde{y}, \tilde{\theta}) < 0\}$	$\mathbf{l}^{(1)} = \{(\tilde{y}, \tilde{\theta})   \tilde{\theta} \in (-\frac{\pi}{2}, 0), \sigma_L(\tilde{y}, \tilde{\theta}) = 0\},$ $\mathbf{l}^{(2)} = \{(\tilde{y}, \tilde{\theta})   \tilde{\theta} \in (-\pi, -\frac{\pi}{2}), \sigma_L(\tilde{y}, \tilde{\theta}) = 0\},$ $\mathbf{l}^{(3)} = \{(\tilde{y}, \tilde{\theta})   \tilde{\theta} \in (-\frac{3}{2}\pi, -\pi), \sigma_L(\tilde{y}, \tilde{\theta}) = 0\},$ $\mathbf{rl}^{(1.1)} = \{(\tilde{y}, \tilde{\theta})   \tilde{\theta} \in (-\frac{\pi}{2}, 0), \sigma_L(\tilde{y}, \tilde{\theta}) > 0, \sigma_P(\tilde{y}, \tilde{\theta}) \leq 0\}$ $\mathbf{rl}^{(1.2)} = \{(\tilde{y}, \tilde{\theta})   \tilde{\theta} \in [0, \frac{\pi}{2}), \sigma_R(\tilde{y}, \tilde{\theta}) > 0, \sigma_P(\tilde{y}, \tilde{\theta}) \leq 0\}$ $\mathbf{rl}^{(1.3)} = \{(\tilde{y}, \tilde{\theta})   \tilde{\theta} \in [\frac{\pi}{2}, \pi), \sigma_R(\tilde{y}, \tilde{\theta}) > 0, \sigma_P(\tilde{y}, \tilde{\theta}) \leq 0\}$ $\mathbf{rl}^{(2)} = \{(\tilde{y}, \tilde{\theta})   \tilde{\theta} \in (-\frac{3}{2}\pi, -\pi), \sigma_P(\tilde{y}, \tilde{\theta}) > 0, \sigma_L(\tilde{y}, \tilde{\theta}) < 0\}$ $\mathbf{sl} = \{(\tilde{y}, \tilde{\theta})   \tilde{y} > +1, \tilde{\theta} = -\frac{\pi}{2}\}$ $\mathbf{rsl}^{(1)} = \{(\tilde{y}, \tilde{\theta})   \tilde{\theta} \in (-\frac{\pi}{2}, 0), \sigma_P(\tilde{y}, \tilde{\theta}) > 0\}$ $\mathbf{rsl}^{(2)} = \{(\tilde{y}, \tilde{\theta})   \tilde{\theta} \in (0, \frac{\pi}{2}), \sigma_P(\tilde{y}, \tilde{\theta}) > 0\}$ $\mathbf{lsl}^{(1)} = \{(\tilde{y}, \tilde{\theta})   \tilde{\theta} \in (-\pi, -\frac{\pi}{2}), \sigma_L(\tilde{y}, \tilde{\theta}) > 0\}$ $\mathbf{lsl}^{(2)} = \{(\tilde{y}, \tilde{\theta})   \tilde{\theta} \in (-\frac{3}{2}\pi, -\pi), \sigma_L(\tilde{y}, \tilde{\theta}) > 0\}$

**Table 1.** Partition of domain  $\mathcal{D}_{(\tilde{y}, \tilde{\theta})}$ , where  $\sigma_R(\tilde{y}, \tilde{\theta}) = \tilde{y} + 1 - \cos(\tilde{\theta})$  and  $\sigma_L(\tilde{y}, \tilde{\theta}) = \tilde{y} - 1 + \cos(\tilde{\theta})$ .

- *go\_straight*, where  $\omega = 0$
  - *turn\_right*, where  $\omega = -\frac{V}{R}$
  - *turn\_left*, where  $\omega = +\frac{V}{R}$
- (7)

which are chosen as follows

$$[\mathit{go\_straight}, \text{ if } (\tilde{y}, \tilde{\theta}) \in \Omega^0] \wedge [\mathit{turn\_right}, \text{ if } (\tilde{y}, \tilde{\theta}) \in \Omega^-] \wedge [\mathit{turn\_left}, \text{ if } (\tilde{y}, \tilde{\theta}) \in \Omega^+] \quad (8)$$

where the partition  $\Omega^0 \cup \Omega^- \cup \Omega^+$  of domain  $\mathcal{D}_{(\tilde{y}, \tilde{\theta})}$  is defined as in Table 1. In Figure 5 the boundaries between subsets of the partition  $\Omega^0 \cup \Omega^- \cup \Omega^+$  are represented by dotted lines, and the direction of motion, when the reference path is a straight line i.e.  $d = 0$ , is represented by directed curves.

### 3.2 Feedback tracking control for generic path

In this section a hybrid feedback controller which solves Problem 1 is derived from the one reported in the previous section. The hybrid model of the vehicle  $PTHA_2$  is characterized by the two modes: *upwards* and *downwards*. In mode *downwards* input  $\omega$  appears with opposite sign with respect to mode *upwards*. Since the controller modes in (8) has been set assuming an upwards binormal axis then, the controller modes *turn\_right* and *turn\_left* have to be switched when the vehicle is in mode *downwards*. Hence, for a generic feasible path  $\Gamma$ , the full-state feedback controller is defined in  $\{\textit{upwards}, \textit{downwards}\} \times \mathcal{D}_{(\tilde{y}, \tilde{\theta})}$  by setting the controller modes as follows

- *go\_straight*, if  $(bin, (\tilde{y}, \tilde{\theta})) \in \{\textit{upwards}, \textit{downwards}\} \times \Omega^0$
  - *turn\_right*, if  $(bin, (\tilde{y}, \tilde{\theta})) \in (\textit{upwards} \times \Omega^-) \vee (bin, (\tilde{y}, \tilde{\theta})) \in (\textit{downwards} \times \Omega^+)$
  - *turn\_left*, if  $(bin, (\tilde{y}, \tilde{\theta})) \in (\textit{upwards} \times \Omega^+) \vee (bin, (\tilde{y}, \tilde{\theta})) \in (\textit{downwards} \times \Omega^-)$
- (9)

where  $\Omega^0$ ,  $\Omega^-$  and  $\Omega^+$  are as in Table 1. The closed-loop hybrid automaton  $CLHA$  obtained by applying the feedback (7),(9) to the vehicle hybrid automaton  $PTHA_2$  is depicted in Figure 4. According to (9) and (8),  $CLHA$  has the discrete state *mode* that assumes values in the set  $\mathcal{O} = \{\textit{zero}, \textit{negative}, \textit{positive}\}$ , as follows

- *mode* = *zero* if  $(\tilde{y}, \tilde{\theta}) \in \Omega^0$
  - *mode* = *negative* if  $(\tilde{y}, \tilde{\theta}) \in \Omega^-$
  - *mode* = *positive* if  $(\tilde{y}, \tilde{\theta}) \in \Omega^+$
- (10)

The initial state  $(mode_0, (\tilde{y}_0, \tilde{\theta}_0))$  of the hybrid automaton  $CLHA$  has to satisfy (10).

The coordinate transformation  $(x, y, \theta) \rightarrow (s, \tilde{y}, \tilde{\theta})$  becomes singular when the vehicle lies on the center of the local osculating circle to the path  $\Gamma$ . That is if, at some time  $\bar{t}$ ,  $\tilde{y}(\bar{t}) |\hat{\kappa}(s(\bar{t}))| = 1$ , or equivalently  $\tilde{y}(\bar{t}) d(\bar{t}) = 1$ . For any initial configuration  $(M(x_0, y_0), \theta_0)$ , with  $M(x_0, y_0) \in \mathcal{T}_\Gamma$  as in (4), the corresponding state  $(\tilde{y}_0, \tilde{\theta}_0)$  satisfies  $\tilde{y}_0 < C^{-1}$ . Further since, by (5)  $d \leq C$ , then  $\tilde{y}_0 d < 1$  at the given initial condition. However, to ensure that

$$\tilde{y} d < 1 \quad \text{i.e.} \quad 1 - \tilde{y} d > 0 \quad (11)$$

will hold along all the trajectories of  $CLHA$ , we need to further restrict the admissible initial vehicle configurations, in terms of its initial orientation  $\theta_0$ .

**Proposition 1.** *Let the continuous disturbance  $d$  be bounded to belong to the interval  $[0, C]$ , with*

$$C < 0.5 . \quad (12)$$

*Then, (11) is satisfied along all trajectories of  $CLHA$  starting from  $(mode_0, (\tilde{y}_0, \tilde{\theta}_0))$  such that*

$$(\tilde{y}_0, \tilde{\theta}_0) \in \mathcal{I}_{(\tilde{y}, \tilde{\theta})} = \left\{ (\tilde{y}, \tilde{\theta}) \in \mathcal{D}_{(\tilde{y}, \tilde{\theta})} \mid |\tilde{y}| < C^{-1} - 1 + |\cos(\tilde{\theta})| \right\} \quad (13)$$

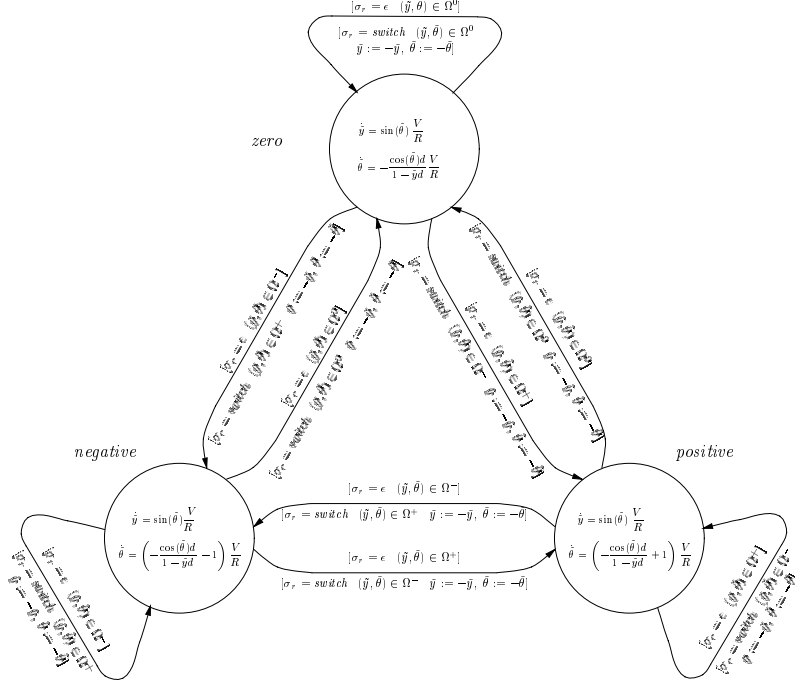


Fig. 4. Hybrid model of the closed-loop system  $CLHA$ .

*Proof.* The proof is not reported due to space limitation.

Note that, for initial configurations satisfying (13) we have  $M(x_0, y_0) \in \mathcal{T}_\Gamma$  as in (4). By Proposition 1, if a reference path  $\Gamma$  has minimum radius of curvature  $R_\Gamma$  greater than twice the minimum turning radius  $R$  of the vehicle, and if no change on the sign of the curvature occurs, then for any initial vehicle configuration  $(M(x_0, y_0), \theta_0)$ , with lateral position and orientation errors bounded to belong to  $\mathcal{I}_{(\tilde{y}, \tilde{\theta})}$  as in (13), condition (11) is ensured.

#### 4 Verification of the hybrid path-tracking controller

In this section the behavior of the hybrid automaton  $CLHA$  is analyzed by introducing an equivalence relation  $\sim$  in the hybrid state space  $\mathcal{O} \times \mathcal{D}_{(\tilde{y}, \tilde{\theta})}$  and by computing the corresponding quotient (see [5]). Consider the partition  $\Pi_{(\tilde{y}, \tilde{\theta})}$  of the domain  $\mathcal{D}_{(\tilde{y}, \tilde{\theta})}$  in (6) given by the 24 subsets  $\{\mathbf{r}^{(1)}, \dots, \mathbf{r}\mathbf{l}^{(2)}\mathbf{l}^{(3)}, \dots, \mathbf{ls}\mathbf{l}^{(2)}, \mathbf{O}\}$ , defined in Table 1, with  $\mathbf{r}\mathbf{l}^{(2)}$  and  $\mathbf{l}^{(3)}$  replaced by  $\mathbf{r}\mathbf{l}^{(2)}\mathbf{l}^{(3)}$ . We say that  $(mode_1, (\tilde{y}_1, \tilde{\theta}_1))$ ,  $(mode_2, (\tilde{y}_2, \tilde{\theta}_2))$  are equivalent, i.e.  $(mode_1, (\tilde{y}_1, \tilde{\theta}_1)) \sim (mode_2, (\tilde{y}_2, \tilde{\theta}_2))$ , iff  $(\tilde{y}_1, \tilde{\theta}_1) \in$



$\mathbf{p}$ , for some  $\mathbf{p} \in \Pi_{(\tilde{y}, \tilde{\theta})}$ , implies  $(\tilde{y}_2, \tilde{\theta}_2) \in \mathbf{p}$ . We associate to the corresponding quotient space  $Q^\sim = \{\mathcal{O} \times \mathbf{r}^{(1)}, \dots, \mathcal{O} \times \mathbf{O}\}$  a nondeterministic finite state machine, referred to as  $FSM_{PTC}$ , with states corresponding to the equivalence classes in  $Q^\sim$  (labeled, with a slight abuse of notation,  $\mathbf{r}^{(1)}, \dots, \mathbf{O}$ ). The next-state function of  $FSM_{PTC}$  is defined as follows: for any  $Q_1, Q_2 \in Q^\sim$ , a transition from  $Q_1$  to  $Q_2$  occurs iff there exists an arc of trajectory of the hybrid automaton  $CLHA$  from some  $(mode_1, (\tilde{y}_1, \tilde{\theta}_1)) \in Q_1$  to some  $(mode_2, (\tilde{y}_2, \tilde{\theta}_2)) \in Q_2$ , for some discrete disturbance  $\sigma_r$  and some continuous disturbance  $d$ .

**Proposition 2.** *Given the hybrid system  $CLHA$ , if the discrete disturbance  $\sigma_r$  takes always the value  $\epsilon$ , then, for any initial hybrid state  $(mode, (\tilde{y}_0, \tilde{\theta}_0)) \in \mathcal{O} \times \mathcal{I}_{(\tilde{y}, \tilde{\theta})}$  as in (13), under the action of any disturbance  $d$  bounded as in (5) with  $C$  as in (12), we have:*

- the quotient system obtained from the equivalence relation  $\sim$  is the finite state machine  $FSM_{PTC}$  depicted in Figure 5;
- an upper bound for the space travelled by the origin of the Frenet’s frame along the path  $\Gamma$ , when the hybrid state is in a given equivalence class is represented by the weight associated to exiting arc;
- the quotient system  $FSM_{PTC}$  remains in each equivalence class a bounded amount of time except for  $\mathbf{O}$  where  $(\tilde{y}, \tilde{\theta}) = (0, 0)$ .

*Proof.* The proof, which is based on reachability analysis, is not reported here due to space limitation.

If the reference path  $\Gamma$  has curvature always of the same sign, the convergence of the Dubins’ car to the path is guaranteed by:

**Corollary 1.** *If the reference path  $\Gamma$  has curvature always of the same sign and amplitude lower than  $\frac{1}{2R}$ , the hybrid feedback control (7) and (9), ensures the tracking of  $\Gamma$  for any initial vehicle configuration in the domain  $\mathcal{I}_{(\tilde{y}, \tilde{\theta})}$  as in (13). The origin of the Frenet frame covers at most a distance of*

$$\begin{cases} 1 + \frac{9}{2}\pi + \frac{\pi}{C} & \text{if } C \in [0, \frac{\pi}{6+5\pi}) \\ 4 + 7\pi + \frac{\pi}{2C} & \text{if } C \in [\frac{\pi}{6+5\pi}, \frac{1}{2}) \end{cases} \quad (14)$$

*along the reference path  $\Gamma$  before the vehicle approaches it with correct orientation.*

*Proof.* The proof is not reported due to space limitation.

By Proposition 2, if  $\Gamma$  is a straight line then the closed-loop system enforces *sliding* motions (see [13] for a tutorial) in the space  $(\tilde{y}, \tilde{\theta})$  on the lines  $\mathbf{sr}$ ,  $\mathbf{sl}$  and the arcs  $\mathbf{r}^{(1)}$ ,  $\mathbf{l}^{(1)}$ ,  $\mathbf{r}^{(3)}$ ,  $\mathbf{l}^{(3)}$  until the origin is reached. If the reference path  $\Gamma$  is not a straight line, sliding motions are enforced only on the lines  $\mathbf{sr}$ ,  $\mathbf{sl}$ , on the arcs  $\mathbf{r}^{(1)}$ ,  $\mathbf{r}^{(3)}$  and on a piece of the arc  $\mathbf{l}^{(3)}$ . Under ideal sliding motion, around the origin the control  $\omega$  switches at infinite frequency between  $\frac{V}{R}$ , 0 and  $-\frac{V}{R}$ . The mean value of such control (i.e. the *equivalent control*) is the signal  $\kappa V$

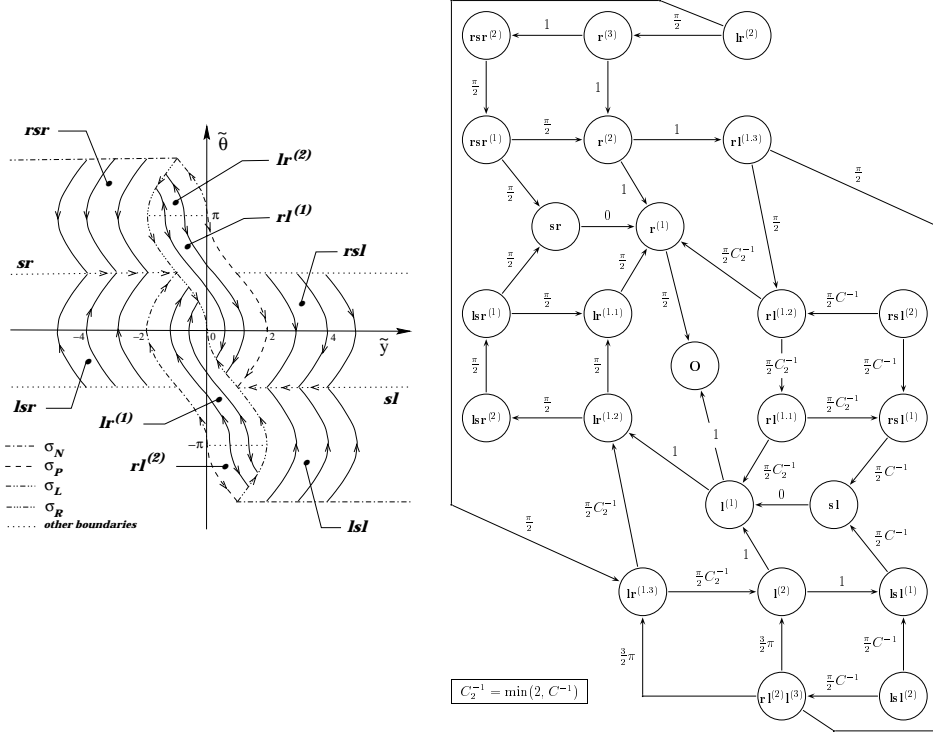


**Fig. 5.** On the left: shortest paths synthesis in the  $(\tilde{y}, \tilde{\theta})$  - plane. On the right: finite state machine  $FSM_{PTC}$  representing the behavior of the closed-loop hybrid system  $CLHA$ , when  $\sigma_r = \epsilon$ .

that makes the robot follows the reference path  $\Gamma$  with velocity  $V$ . In the real implementation smoothing techniques are applied to avoid this chattering.

The behavior of the closed-loop system  $CLHA$  under the action of the discrete disturbance  $\sigma_r$  is characterized by the following propositions.

**Proposition 3.** *Given an initial condition  $(\tilde{y}_0, \tilde{\theta}_0)$  in the open neighborhood of the origin*

$$\mathcal{N}_{(\tilde{y}, \tilde{\theta})} = \left\{ (\tilde{y}, \tilde{\theta}) : |\tilde{y}| < 1, -\arccos\left(\frac{1}{2} - \frac{\tilde{y}}{2}\right) < \tilde{\theta} < \arccos\left(\frac{1}{2} + \frac{\tilde{y}}{2}\right) \right\} \quad (15)$$

(see Figure 6), the hybrid closed-loop system  $CLHA$  keeps the continuous-time trajectory  $(\tilde{y}(t), \tilde{\theta}(t))$  inside  $\mathcal{N}_{(\tilde{y}, \tilde{\theta})}$ , under any disturbance  $d(t)$  bounded as in (5) and any sequence of events  $\sigma_r$ .

*Proof.* The proof is not reported due to space limitation.

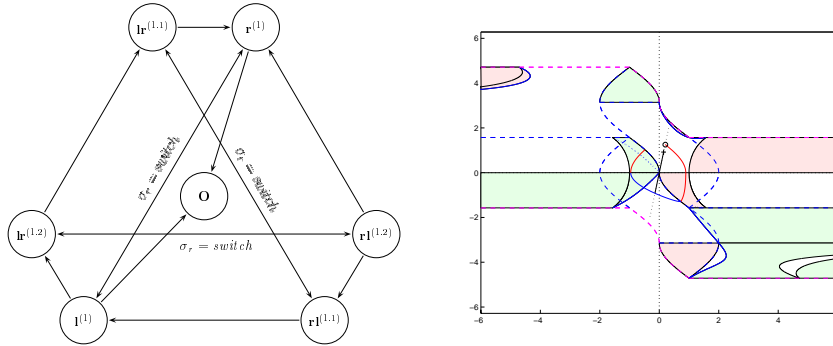


**Fig. 6.** On the left: quotient system  $FSM_{PTC}^D$  representing the behavior of the closed-loop hybrid system  $CLHA$ , when the initial state belongs to  $\mathcal{O} \times \mathcal{N}_{(\tilde{y}, \tilde{\theta})}$ . On the right: regions in the domain  $\mathcal{D}_{(\tilde{y}, \tilde{\theta})}$  where  $\dot{W} > 0$ .

**Proposition 4.** *If the reference path  $\Gamma$  is such that changes in the curvature sign are at distance greater than  $(5 + \frac{\pi}{2})R$  along it, then the hybrid feedback control (7), with modes chosen according to (9) stabilizes the robot along the reference path  $\Gamma$ .*

*Proof.* The set  $\mathcal{N}_{(\tilde{y}, \tilde{\theta})}$  defined in (15) is such that

$$\mathcal{N}_{(\tilde{y}, \tilde{\theta})} \subset \mathbf{O} \cup \mathbf{r}^{(1)} \cup \mathbf{l}^{(1)} \cup \mathbf{lr}^{(1,1)} \cup \mathbf{lr}^{(1,2)} \cup \mathbf{rl}^{(1,1)} \cup \mathbf{rl}^{(1,2)}.$$

Since, by Proposition 3,  $\mathcal{N}_{(\tilde{y}, \tilde{\theta})}$  is a robust invariant set for the closed-loop hybrid system  $CLHA$ , then, if we restrict our attention to the domain  $\mathcal{N}_{(\tilde{y}, \tilde{\theta})}$ , the transitions from  $\mathbf{lr}^{(1,2)}$  to  $\mathbf{lsr}^{(2)}$  and from  $\mathbf{rl}^{(1,1)}$  to  $\mathbf{rsl}^{(1)}$  in the quotient system  $FSM_{PTC}$  should be removed. Furthermore, notice that, under the action of the discrete disturbance  $\sigma_r = switch$ , the reset  $\tilde{y} := -\tilde{y}$  and  $\tilde{\theta} := -\tilde{\theta}$  introduces the mutual transitions  $\mathbf{r}^{(1)} \leftrightarrow \mathbf{l}^{(1)}$ ,  $\mathbf{lr}^{(1,1)} \leftrightarrow \mathbf{rl}^{(1,1)}$ , and  $\mathbf{lr}^{(1,2)} \leftrightarrow \mathbf{rl}^{(1,2)}$ . Hence, in the presence of the discrete disturbance  $\sigma_r$  and for any disturbance  $d$  as in (5), when the initial state belongs to  $\mathcal{O} \times \mathcal{N}_{(\tilde{y}, \tilde{\theta})}$ , the quotient system  $FSM_{PTC}^D$  obtained from the equivalent relation  $\equiv$  is as in Figure 6.

To analyse the convergence to  $\mathbf{O}$  of trajectories  $(\tilde{y}(t), \tilde{\theta}(t))$ , introduce the function

$$W(\tilde{y}, \tilde{\theta}) = \frac{1}{2}(\tilde{y}^2 + \tilde{\theta}^2). \quad (16)$$

$W(\tilde{y}, \tilde{\theta})$  has the property that if, at time  $t = \bar{t}$ ,  $\sigma_r = switch$  then  $W(\tilde{y}(\bar{t}), \tilde{\theta}(\bar{t})) = W(\tilde{y}(\bar{t}^-), \tilde{\theta}(\bar{t}^-))$ . The derivative with respect to time of function (16) evaluates to

$$\dot{W}(\tilde{y}, \tilde{\theta}) = \left[ \tilde{y} \sin(\tilde{\theta}) - \tilde{\theta} \frac{\cos(\tilde{\theta})d}{1 - \tilde{y}d} - \tilde{\theta} \varpi \right] \frac{V}{R}, \quad (17)$$

where  $\varpi = 0, -1$ , and  $1$  in mode *zero*, *negative*, and *positive*, respectively. The study of the sign of  $\dot{W}(\tilde{y}, \tilde{\theta})$  is extended to the entire domain  $\mathcal{D}_{(\tilde{y}, \tilde{\theta})}$ . Under assumption (11), multiplying (17) by  $\frac{R}{V}(1 - \tilde{y}d)$ , we have

$$\dot{W} > 0 \quad \leftrightarrow \quad \mu(\tilde{y}, \tilde{\theta}) = d \left[ -\tilde{y}^2 \sin(\tilde{\theta}) - \tilde{\theta} \cos(\tilde{\theta}) + \varpi \tilde{y} \tilde{\theta} \right] + \left[ \tilde{y} \sin(\tilde{\theta}) - \varpi \tilde{\theta} \right] > 0$$

for some disturbance  $d$  bounded as in (5). Hence, for any  $(\tilde{y}, \tilde{\theta})$  such that

$$\eta_1(\tilde{y}, \tilde{\theta}) = \tilde{y} \sin(\tilde{\theta}) - \varpi \tilde{\theta} > 0$$

there exists  $d$  as in (5) such that  $\mu(\tilde{y}, \tilde{\theta}) > 0$  and  $\dot{W} > 0$ . Otherwise, if  $(\tilde{y}, \tilde{\theta})$  is such that  $\eta_1(\tilde{y}, \tilde{\theta}) < 0$ , then there exists  $d$  as in (5) such that  $\dot{W} > 0$  if and only if  $\mu(\tilde{y}, \tilde{\theta})$  is positive for  $d = 1$ . That is, if

$$\eta_2(\tilde{y}, \tilde{\theta}) = -\sin(\tilde{\theta})\tilde{y}^2 + \left[ \sin(\tilde{\theta}) + \varpi \tilde{\theta} \right] \tilde{y} - \left[ \tilde{\theta} \cos(\tilde{\theta}) + \varpi \tilde{\theta} \right] > 0,$$

which can be solved for  $\tilde{y}$  given  $\tilde{\theta}$ . The regions in the domain  $\mathcal{D}_{(\tilde{y}, \tilde{\theta})}$  where the function (16) locally increases are reported in Figure 6. Such regions are delimited by curves  $\eta_1(\tilde{y}, \tilde{\theta}) = 0$  and  $\eta_2(\tilde{y}, \tilde{\theta}) = 0$ , where  $\varpi = 0, -1$  and  $1$  if  $(\tilde{y}, \tilde{\theta}) \in \Omega^0, \Omega^-,$  and  $\Omega^+$ , respectively. By (17), the continuous disturbance  $d$  which maximizes  $\dot{W}(t)$  is

$$d^* = \begin{cases} 1 & \text{if } \tilde{\theta} \cos(\tilde{\theta}) < 0 & \text{i.e. } \tilde{\theta} \in \left(-\frac{\pi}{2}, 0\right) \cup \left(\frac{\pi}{2}, \frac{3}{2}\pi\right) \\ 0 & \text{if } \tilde{\theta} \cos(\tilde{\theta}) > 0 & \text{i.e. } \tilde{\theta} \in \left(-\frac{3}{2}\pi, -\frac{\pi}{2}\right) \cup \left(0, \frac{\pi}{2}\right) \end{cases} \quad (18)$$

Consider an initial condition  $(\tilde{y}_0, \tilde{\theta}_0)$  in a neighborhood of the origin and in region  $\mathcal{N}_{(\tilde{y}, \tilde{\theta})} \cap \mathbf{r}^{\mathbf{1},2}$ . At the initial time, the hybrid model *CLHA* is in mode *negative*. Let us assume that  $\sigma_r = \epsilon$ , for the moment, and let us analyse the evolution of the hybrid model *CLHA* under the action of the continuous disturbance  $d$ . Under the action of the worst disturbance (18), the trajectory  $(\tilde{y}(t), \tilde{\theta}(t))$  originating from  $(\tilde{y}_0, \tilde{\theta}_0)$  reaches the curves  $\mathbf{r}^{\mathbf{1}}$ . First  $W(t)$  decreases (in  $\mathbf{r}^{\mathbf{1},2}$ ), then it increases (in  $\mathbf{r}^{\mathbf{1},1}$ ). Hence, *mode* switches to *positive*.  $W(t)$  decreases (in the first part of  $\mathbf{r}^{\mathbf{1},2}$ ), and it increases again later on (in  $\mathbf{r}^{\mathbf{1},2}$  and  $\mathbf{r}^{\mathbf{1},1}$ ) until  $(\tilde{y}(t), \tilde{\theta}(t))$  reaches  $\mathbf{r}^{\mathbf{1}}$ . Finally, following a sliding motion along the curve  $\mathbf{r}^{\mathbf{1}}$ ,  $(\tilde{y}(t), \tilde{\theta}(t))$  reaches the origin.

Along this trajectory  $W(t)$  assume two local maxima, which correspond to the intersections of  $\mathbf{l}^{\mathbf{1}}$  and  $\mathbf{r}^{\mathbf{1}}$ , and two local minima: the first on the line  $\tilde{\theta} = 0$  when  $\tilde{y} > 0$ , and the second inside region  $\mathbf{r}^{\mathbf{1},2}$ . Let  $\delta = \|(\tilde{y}_0, \tilde{\theta}_0)\|$ . Since the trajectory  $(\tilde{y}(t), \tilde{\theta}(t))$  is continuous with respect to the initial condition  $(\tilde{y}_0, \tilde{\theta}_0)$ , then there exist two continuous functions  $\zeta_{\max}, \zeta_{\min} : \mathbb{R} \rightarrow \mathbb{R}$  such that

$$\max_d \max_t \|(\tilde{y}(t), \tilde{\theta}(t))\| = \zeta_{\max}(\delta) \quad \text{and} \quad \min_d \min_t \|(\tilde{y}(t), \tilde{\theta}(t))\| = \zeta_{\min}(\delta) \quad (19)$$

Further, since the local maximum and minimum points tend to the origin as  $\|(\tilde{y}_0, \tilde{\theta}_0)\|$  tends to zero, then  $\lim_{\delta \rightarrow 0} \zeta_{\max}(\delta) = 0$  and  $\lim_{\delta \rightarrow 0} \zeta_{\min}(\delta) = 0$ .

Suppose now that a discrete disturbance  $\sigma_r = \textit{switch}$  occurs at the precise time  $\bar{t}$  at which  $(\tilde{y}(\bar{t}^-), \tilde{\theta}(\bar{t}^-))$  is opposite to  $(\tilde{y}_0, \tilde{\theta}_0)$  with respect to the origin. Then, the state  $(\tilde{y}(\bar{t}^-), \tilde{\theta}(\bar{t}^-))$  is reset to  $(\tilde{y}(\bar{t}), \tilde{\theta}(\bar{t})) = (-\tilde{y}(\bar{t}^-), -\tilde{\theta}(\bar{t}^-)) \in \mathcal{N}_{(\tilde{y}, \tilde{\theta})}$ , which lies on the same line to the origin of  $(\tilde{y}_0, \tilde{\theta}_0)$ . If  $W(\tilde{y}_0, \tilde{\theta}_0) > W(\tilde{y}(\bar{t}), \tilde{\theta}(\bar{t})) = W(-\tilde{y}(\bar{t}^-), -\tilde{\theta}(\bar{t}^-))$  then the convergence is preserved. But, if  $W(\tilde{y}_0, \tilde{\theta}_0) < W(\tilde{y}(\bar{t}), \tilde{\theta}(\bar{t})) = W(-\tilde{y}(\bar{t}^-), -\tilde{\theta}(\bar{t}^-))$  then, under the action of the discrete disturbance  $\sigma_r = \textit{switch}$ , the state  $(\tilde{y}, \tilde{\theta})$  is reset to a point farther away from the origin than the initial state  $(\tilde{y}_0, \tilde{\theta}_0)$  and convergence can be lost.

However, if the reference path  $\Gamma$  is such that changes in the curvature sign are at a distance greater than  $(5 + \frac{\pi}{2})R$  along it, between two successive actions of the discrete disturbance  $\sigma_r$ , the state  $(\tilde{y}, \tilde{\theta})$  has enough time to reach the origin. In fact, assuming that, in the worst case,  $(\tilde{y}(\bar{t}), \tilde{\theta}(\bar{t})) \in \mathcal{N}_{(\tilde{y}, \tilde{\theta})} \cap \mathbf{r}\mathbf{l}^{(1,2)}$ , an upper bound on the length the arc of  $\Gamma$  spanned by the origin of the Frenet frame as  $(\tilde{y}(t), \tilde{\theta}(t))$  converges to the origin, is given by  $L(\mathbf{r}\mathbf{l}^{(1,2)}) + L(\mathbf{r}\mathbf{l}^{(1,1)}) + L(\mathbf{l}^{(1)}) + L(\mathbf{l}^{(1,2)}) + L(\mathbf{l}^{(1,1)}) + L(\mathbf{l}^{(1)})$  that, according to the weighted *FSM PTC* reported in Figure 5, evaluates to  $(5 + \frac{\pi}{2})R$ .

To prove the robust stabilization of the robot along the reference path  $\Gamma$  we have to show that for any  $\epsilon > 0$ , there exists  $\delta > 0$  such that any trajectory  $(\tilde{y}(t), \tilde{\theta}(t))$  of the hybrid system *CLHA*, originating from any  $(\tilde{y}_0, \tilde{\theta}_0)$  with  $\|(\tilde{y}_0, \tilde{\theta}_0)\| < \delta$ , we have  $\|(\tilde{y}(t), \tilde{\theta}(t))\| < \epsilon$ . Given any  $\epsilon > 0$ , consider any initial condition  $(\tilde{y}_0, \tilde{\theta}_0)$  with

$$\|(\tilde{y}_0, \tilde{\theta}_0)\| \leq \delta = \zeta_{\max}^{-1}(\zeta_{\min}^{-1}(\zeta_{\max}^{-1}(\epsilon))). \quad (20)$$

The trajectory  $(\tilde{y}(t), \tilde{\theta}(t))$  evolves inside a ball of radius  $\zeta_{\min}^{-1}(\zeta_{\max}^{-1}(\epsilon))$ . If a disturbance  $\sigma_r = \textit{switch}$  occurs at some time  $\bar{t}$ , then the state is reset to  $(\tilde{y}(\bar{t}), \tilde{\theta}(\bar{t})) = (-\tilde{y}(\bar{t}^-), -\tilde{\theta}(\bar{t}^-)) \in \mathcal{N}_{(\tilde{y}, \tilde{\theta})}$ . In the evolution for  $t > \bar{t}$  the trajectory reaches the origin before a further discrete disturbance will show up. Moreover, since  $\|(\tilde{y}(\bar{t}), \tilde{\theta}(\bar{t}))\| \leq \zeta_{\min}^{-1}(\zeta_{\max}^{-1}(\epsilon))$  then, the trajectory  $(\tilde{y}(t), \tilde{\theta}(t))$  for  $t > \bar{t}$  does not exit a ball of radius  $\zeta_{\max}^{-1}(\zeta_{\min}^{-1}(\epsilon)) = \epsilon$ . Then, the hybrid feedback control (7), with modes chosen according to (9) robustly stabilizes the robot along the reference path  $\Gamma$ .

## 5 Conclusions

In this paper, we have used modern techniques developed for hybrid systems simulation and verification to solve and prove stability of a control technique for an interesting problem, that is route tracking by nonholonomic vehicles with bounds on the curvature and limited sensory information. The proposed controller is reminiscent of a synthesis proposed elsewhere for an optimal control problem to track straight routes, whose generalization to generic routes turned out to be difficult to analyze otherwise. We believe that this case study, besides its intrinsic interest in applications, also has a value in showing the potential of hybrid systems analysis techniques as applied to complex control problems.

## References

1. E. Asarin, T. Dang, O. Maler, and O. Bournez. Approximate reachability analysis of piecewise-linear dynamical systems. In Nancy Lynch and Bruce H. Krogh, editors, *Third International Workshop, HSCC2000, Hybrid Systems: Computation and Control*, volume 1790 of *Lecture Notes in Computer Science*, pages 20–31. Springer-Verlag, New York, U.S.A., 2000.
2. A. Balluchi, L. Benvenuti, M. D. Di Benedetto, C. Pinello, and A. L. Sangiovanni-Vincentelli. Automotive engine control and hybrid systems: Challenges and opportunities. *Proceedings of the IEEE*, 88, "Special Issue on Hybrid Systems" (invited paper)(7):888–912, July 2000.
3. A. Balluchi, L. Benvenuti, H. Wong-Toi, T. Villa, and A. L. Sangiovanni-Vincentelli. Controller synthesis for hybrid systems with lower bounds on event separation. In *Proc. 38th IEEE Conference on Decision and Control*, pages 3984–3989, Phoenix, Arizona, USA, December 1999.
4. L. E. Dubins. On curves of minimal length with a constraint on average curvature and with prescribed initial and terminal positions and tangents. *American Journal of Mathematics*, 79:497–516, 1957.
5. Thomas A. Henzinger. Hybrid automata with finite bisimulations. In Z. Fülöp and F. Gécseg, editors, *ICALP'95: Automata, Languages, and Programming*, pages 324–335. Springer-Verlag, 1995.
6. J.P. Laumond, S. Sekhavat, and F. Lamiroux. *Robot motion planning and control*. Springer-Verlag, Berlin, Germany, 1998.
7. J. Lygeros, C. Tomlin, and S. Sastry. Controllers for reachability specifications for hybrid systems. *Automatica*, 35(3), March 1999.
8. A. Olivero, J. Sifakis, and S. Yovine. Using abstractions for the verification of linear hybrid systems. In *Proceedings of Sixth International Conference on Computer-Aided Verification (CAV-94)*, pages 81–94. Springer-Verlag, 1994. Lecture Notes in Computer Science 818.
9. C. Samson. Control of chained systems application to path following and time-varying point-stabilization of mobile robots. *IEEE Transaction on Automatic Control*, 40(1):64–77, January 1995.
10. O.J. Sordalen and C. Canudas de Wit. Exponential control law for a mobile robot: Extension to path following. *IEEE Transactions on Robotics and Automation*, 9(6):837–842,, 1993.
11. P. Souères, A. Balluchi, and A. Bicchi. Optimal feedback control for line tracking with a bounded-curvature vehicle. to appear in *International Journal of Control*, 2000.
12. D. Tilbury, O.J. Sordalen, L. Bushnell, and S.S. Sastry. A multi-steering trailer system: conversion into chained form using dynamic feedback. *IEEE Transactions on Robotics and Automation*, 11(6):807–18, December 1995.
13. V.I. Utkin. Variable structure systems with sliding modes: a survey. *IEEE Transactions on Automatic Control*, 22:212–222, 1977.
14. J. Zhang, K. H. Johansson, J. Lygeros, and S. Sastry. Dynamical systems revisited: Hybrid systems with zeno executions. In Nancy Lynch and Bruce H. Krogh, editors, *Third International Workshop, HSCC2000, Hybrid Systems: Computation and Control*, volume 1790 of *Lecture Notes in Computer Science*, pages 451–464. Springer-Verlag, New York, U.S.A., 2000.